

RESEARCH ARTICLE

## Synthesis and Antibacterial studies of Lanthanum, Cerium and Erbium loaded Copper Oxide Nanoparticles

R Sasikala<sup>1</sup>, \*S Kutti Rani<sup>1</sup>, K Karthikeyan<sup>1</sup>, D Easwaramoorthy<sup>1</sup>

<sup>1</sup>Department of Chemistry, B. S. Abdur Rahman University, Vandalur, Chennai-600048, India.

Received- 20 August 2016, Revised- 23 September 2016, Accepted- 30 October 2016, Published- 5 November 2016

### ABSTRACT

Field Emission Scanning Electron Microscopy (FESEM), X-ray Diffraction (XRD) and Energy Dispersive Spectra (EDS) were employed to synthesise and characterize Lanthanum, Cerium and Erbium loaded CuO nanoparticles (LCO, CCO and ECO NPs). The nanoparticles were explored for the antibacterial activity against the human pathogenic bacteria such as Salmonella typhimurium, Escherichia coli, Proteus mirabilis, Pseudomonas aeruginosa, Acinetobacter baumannii and Klebsiella pneumonia by the standard well diffusion method using amoxicillin as the standard. The nanoparticles exhibited excellent antibacterial activity against the growth of microorganisms. The Minimum Inhibitory Concentration (MIC) of the existing bacterial strains was also determined.

**Keywords:** CuO nanoparticles, Rare earth metal loaded CuO nanoparticles, Antibacterial activity, Well diffusion assay, Minimum inhibitory concentration.

### 1. INTRODUCTION

In recent times considerable effort has been given for the synthesis of nanomaterials [1] due to their applications in the field of nanoelectronics [2], nanosensors [3], storage materials [4], catalysis and nano-medicine [5]. Among the various applications, there is a rising demand for new antimicrobial materials for disinfection applications. In this scenario, nanomaterials are principally important, owing to an elevated surface-to-volume ratio, which offer a large active surface in contact with the microorganisms [6]. Commonly used antimicrobial nanoparticles containing silver [7], magnesium oxide [8], copper oxide [9], iron oxide [10], zinc oxide [11], nickel oxide [12] and titanium dioxide [13] NPs are explored. Among the various metal oxide NPs, CuO is documented as a good, non-toxic, more stable, insoluble in most of the organic solvents, readily stored and less expensive antimicrobial agent [14]. The bactericidal properties of CuO NPs depend on their size, stability, surface area, morphology and concentration. Since, pure CuO is not effective, the modification of CuO with transition metals / rare earth metals is now an

excellent area for developing photocatalytic and electronic applications [15-17].

The rare earth metals have gained huge attention due to their unique optical characteristics, especially as a fluorophore in a variety of biological applications [18, 19]. Additionally, these elements provide good anticoagulant, antibacterial, anti-cancer, anti-inflammatory and anti-tumor biological capabilities [20–28]. The commonly used lanthanide ions for doping are Pr<sup>3+</sup>, Er<sup>3+</sup>, Sm<sup>3+</sup>, Eu<sup>3+</sup>, Ce<sup>3+</sup>, Tb<sup>3+</sup>, Dy<sup>3+</sup>, Nd<sup>3+</sup>, Yb<sup>3+</sup> and Tm<sup>3+</sup> [29]. Hence, we report the synthesized rare earth metals loaded CuO NPs such as LCO, CCO and ECO NPs and their potential antimicrobial activity.

### 2. EXPERIMENTAL

#### 2.1. Materials and methods

Copper nitrate pentahydrate (Aldrich 99%), oxalic acid dehydrate (Merck 99%), Ce(NH<sub>4</sub>)<sub>4</sub>(SO<sub>4</sub>)<sub>4</sub>.2H<sub>2</sub>O (Spectrochem 98.7%), lanthanum(III) nitrate hexahydrate (Aldrich 99%) and erbium (III) chloride hexahydrate (Aldrich 99.9%) were used as received. The experimental solution was prepared using distilled water.

\*Corresponding author. Tel.: +91944206191

Email address: [skrani@bsauniv.ac.in](mailto:skrani@bsauniv.ac.in) (S.K.Rani)

Double blind peer review under responsibility of DJ Publications

<http://dx.doi.org/10.18831/djchem.org/2016041004>

2455-5193 © 2016 DJ Publications by Dedicated Juncture Researcher's Association. This is an open access article under the CC BY-NC-ND license (<http://creativecommons.org/licenses/by-nc-nd/4.0/>).

Powder X-ray diffraction patterns were obtained using X'Per PRO diffractometer equipped with a  $\text{CuK}\alpha$  radiation (wavelength  $1.5406\text{\AA}$ ) at 2.2 kWMax. Peak positions were compared with the standard files to identify the crystalline phase. The morphology of the catalyst was examined using a JEOL JSM-6701F cold Field Emission Scanning Electron Microscope (FE-SEM) equipped with OXFORD Energy Dispersive X-ray Spectrum (EDS). All chemicals and Petri plates used for microbial studies were procured from HiMedia, Ltd, Mumbai, India.

## 2.2. Preparation of rare earth metal (La, Ce, Er) loaded CuO NPs

Aqueous solutions of 100mL of 0.4M copper nitrate pentahydrate and 100mL of 0.6M oxalic acid were heated to  $90^\circ\text{C}$  separately. The oxalic acid solution was added to copper nitrate solution and copper oxalate was precipitated. A solution of 0.122g of  $\text{Ce}(\text{NH}_4)_4(\text{SO}_4)_4$  in 5mL of water was added to this mixture, heated to  $60\text{--}80^\circ\text{C}$  and stirred for 1h. The solution was cooled to room temperature. The Ce with copper oxalate mixture was washed several times with distilled water, dried at  $100^\circ\text{C}$  for 5h and calcination of the mixed precipitate at  $450^\circ\text{C}$  for 5 h decomposed copper oxalate to CuO NPs. The Ce loaded CuO NPs was collected and used for further analysis. These NPs contained 1 wt% of Ce. The bare CuO NPs were prepared without addition of  $\text{Ce}(\text{NH}_4)_4(\text{SO}_4)_4$  by the same procedure mentioned in figure 1. Er loaded CuO were also prepared by the same procedure with respective precursors.

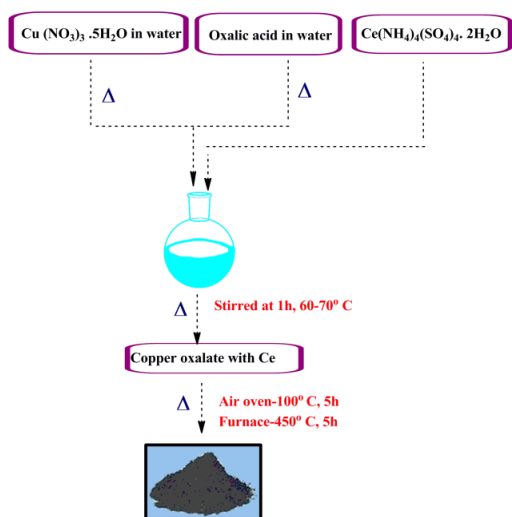


Figure 1. Schematic representation for the preparation of Ce loaded CuO NPS

## 2.3. Antibacterial activity by well diffusion method

Antibacterial activities of the synthesized NPs were tested against gram-negative bacterial strains. The following bacterial strains *Escherichia coli* ATCC 25922, *Pseudomonas aeruginosa* ATCC 27853, *Salmonella typhimurium* ATCC 14028, *Proteus mirabilis* ATCC 35659, *Acetobacter baumannii* ATCC 19606 and *Klebsiella pneumoniae* ATCC 35657 were purchased from the American type culture collection and used to determine the antibacterial activity using well diffusion method. The results were interpreted based on CLSI (Clinical and Laboratory Standards Institute) standard tables.

The synthesised NPs was dissolved in sterile double distilled water and sonicated. The bacterial strains *E.coli*, *P.aeruginosa*, *S.typhimurium*, *P.mirabilis*, *A.baumannii* and *K.pneumonia* were grown in nutrient broth for 24h at  $37^\circ\text{C}$ . A  $100\mu\text{l}$  nutrient broth culture of each bacterial organism was used to prepare bacterial lawns. The wells in each plate were loaded with  $100\mu\text{l}$  of different CuO NPs suspension i.e. bare CuO, LCO, CCO and ECO NPs. Amoxicilline was used as a control. The results were attained when a zone of inhibition was noticed around the well after the incubation.

## 2.4. Minimum Inhibitory Concentration (MIC)

Minimum inhibitory concentrations (MIC) of NPs were tested in *E.coli*, *P.aeruginosa*, *S. typhimurium*, *P.mirabilis*, *A.baumannii* and *K.pneumonia* by the micro agar dilution method. A stock solution of La/Ce/Er CuO NPs was prepared by dissolving 5mg of the compound in 1mL of distilled water and sonicated. The colour of solution changed to black due to nano dispersion in solution. The NPs solution was serially diluted to give concentrations in the range of 512, 256, 128, 64, 32, 16 and  $8\mu\text{g}/\text{mL}$ . Similarly, the standard solution of amoxycillin was arranged at the same concentration.

The methodology includes a series of 96 microtiter plates for determining the antibacterial activity of the NPs. The first assay tube, which contains  $100\mu\text{l}$  broth was added with  $256\mu\text{g}/\text{mL}$  NPs test solution and mixed thoroughly. From that  $100\mu\text{l}$  of the suspension was pipetted out and added into the second assay tube and was mixed thoroughly. This

type of dilution was repeated upto 8µg/mL. The racks of plates were placed inside the incubator at 37 °C for 24 h. After the incubation period, the assay concentrations were again streaked into nutrient agar plate due to drug-microorganism mixture. The lowest concentration of the test compounds, which caused apparently a complete inhibition of growth of organism, was taken as minimum inhibitory concentration. The bare CuO NPs were also tested for comparison.

### 3. RESULTS AND DISCUSSION

#### 3.1. Catalyst characterization

Preparation, characterization and the catalytic activity of LCO NPs were reported earlier by our group [30]. The prepared Ce and Er loaded CuO NPs was characterized by FE-SEM, XRD, and EDS analysis. The powder XRD patterns identified the crystalline nature of the bare CuO NPs as shown in figure 2. The diffraction peaks  $2\theta$  are 35.45°, 38.73°, 42.50°, 48.92°, 61.99° and 66.49° corresponding to (hkl) values as (002), (111), (200), (202), (220) and (113) which are found to be same for single phase CuO NPs with a monoclinic (Figure 2a) (standard JCPDS File No: 048-1548) [31]. In the XRD spectrum of CCO system shown in figure 2b, at the  $2\theta$  values of 28.90 which corresponds to the (111) plane [32] of  $Ce^{4+}$  (JCPDS 898436) the presence of one new sharp peak is found in comparison with the bare CuO NPs. Figure 2c represents ECO NPs. From figure 3 it is clear that the corresponding peaks of CCO and ECO NPs was marginally shifted to lower angle, which exposed the loading of metals on the CuO surface [33]. Scherrer formula as shown in (3.1) was applied to determine the CuO, CCO and ECO NPs crystalline size.

$$D = \frac{K\lambda}{\beta \cos\theta} \quad (3.1)$$

where D is the catalyst crystal size, K represents the dimensionless constant,  $\lambda$  is the X-ray wavelength,  $\beta$  is the full width at half-maximum (FWHM) of the diffraction peak,  $2\theta$  represents the diffraction angle and  $\theta$  is the Bragg angle. On the basis of this equation the crystalline size of LCO (19 nm), CCO (18 nm), ECO (16 nm) were obtained which were lower than bare CuO (25 nm).

The FE-SEM images of CCO and ECO NPs are shown in figure B1. It is revealed

that the particles are concentrated in the nanometer region. Moreover on the basis of scherrer's formula they are in close agreement with grain size. Figure B1 (a & b) shows that there is almost uniform formation of spherical shaped CCO (3µm) and ECO (2µm) particle with aggregation.

The EDS spectra in figure B2 revealed the Cu and O presence together with the peaks of the related metal ions such as Ce and Er in figure B2( b and c) in the structure of the NPs. This confirmed the successful loading of metal ions on the CuO NPS surface.

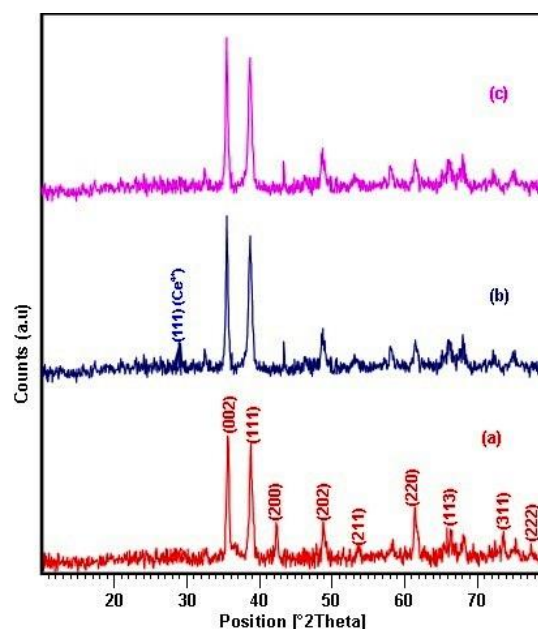


Figure 2. XRD patterns of a) pure CuO, b) CCO and c) ECO NPs

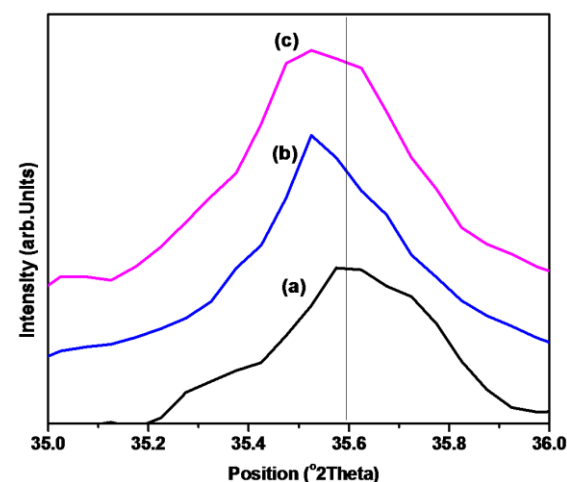


Figure 3. Shows magnification of XRD patterns of a) pure CuO, b) CCO and c) ECO NPs

#### 3.2. Antibacterial Activity of rare earth metal (La, Ce, Er) loaded CuO NPs.

Antibacterial activity of rare earth metal (La, Ce and Er) loaded CuO NPs was investigated against various bacterial strains, such as E.coli, S.typhimurium, P.aeruginosa, P.mirabilis, A.baumannii and K.pneumoniae in a well diffusion assay method. The zone of inhibition values of each bacterial agent (LCO, CCO and ECO) against tested bacterial strains are provided in table A1.

The antibacterial activity of LCO, CCO, ECO NPs (Figure 4) exhibited maximum zone of inhibition against a range of bacteria except P.aeruginosa and A.baumannii than pure CuO NPs. It revealed that the loaded metal ions entrenched into CuO and its particles cooperatively restrain the bacteria [34]. From this point of view, the LCO, CCO, ECO NPs shows highest activity against E. coli, S. typhimurium, P.mirabilis than pure CuO NPs while minimum activity against K.pneumonia [35, 36, 37]. No zone of inhibition was observed for P.aeruginosa and A. baumannii.

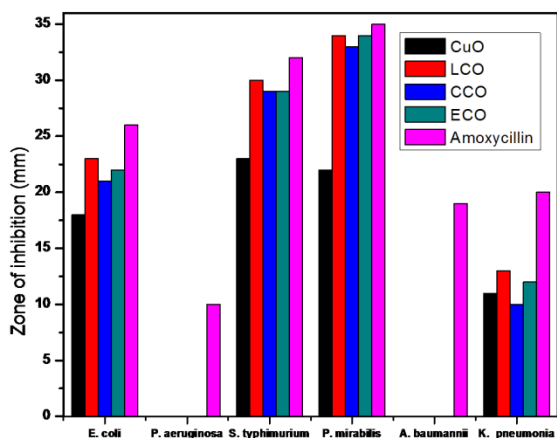


Figure 4. Antibacterial activity of CuO, LCO, CCO and ECO NPs against pathogenic microbes

The minimum inhibitory concentrations (MIC) of the synthesized NPs against the organism under test comes in the range of 70-256  $\mu\text{g/ml}$  are listed in table A2. The result showed that the rare earth metal loaded CuO NPs are more effective against E.coli, S.typhimurium, P.mirabilis strains MIC at 70-80  $\mu\text{g/ml}$ , while the rest of the other organism such as K.pneumonia in the range of 180-200  $\mu\text{g/ml}$  and P.aeruginosa, A.baumannii of MIC at 256  $\mu\text{g/ml}$ . The MIC of CuO NPs against all the six bacteria are above 200  $\mu\text{g/ml}$ , which points towards the fact that pure CuO NPs are very weak when compared to all the bacteria tested.

These results suggested that the La/Ce/Er loaded CuO NPs have commendable antibacterial activities towards E.coli, S.typhimurium and P. mirabilis, but have lower antibacterial activities to K. pneumonia. No activity was observed for P.aeruginosa, A.baumannii. Eventhough the appropriate antibacterial mechanism of nanomaterials is unknown, it is evident that the morphology or large surface area of NPs can immensely affect the antibacterial activity.

#### 4. CONCLUSION

Novel rare earth metal (La, Ce and Er) loaded CuO nanoparticles were prepared with increased surface area via simple precipitation thermal decomposition method. The synthesized material was confirmed by FESEM, XRD and EDS analysis. The average crystalline size of rare earth metal loaded CuO (16-19 nm) was observed. It is lower than that of CuO NPs and the elements present in the NPs were confirmed by EDS analysis. Additionally, the LCO, CCO and ECO nanoparticles are described as a potential entrant for bactericidal applications and current practical alternative for the improvement of fresh bactericides due to cost, abundant resources, high surface area and smaller particle size.

#### ACKNOWLEDGEMENTS

The authors are grateful to the DST-SERB (Project no. SB/FT/CS-033/2013) for financial support and School of Life Science, B.S.Abdur Rahman University for bacterial studies. One of the authors R.Sasikala thanks B S Abdur Rahman University for providing a fellowship.

#### REFERENCES

- [1] M.F.Garcia, A.M.Arias and J.C.Hanson, Nanostructured Oxides in Chemistry: Characterization and Properties, Chemical Reviews, Vol. 104, No. 9, 2004, pp. 4063–4104, <http://dx.doi.org/10.1021/cr030032f>.
- [2] M.J.Deen and F.Pascal, Electrical Characterization of Semiconductor Materials and Devices-Review, Journal of Materials Science: Materials in Electron, Vol. 17, No. 8, 2006, pp. 549–575, <http://dx.doi.org/10.1007/s10854-006-0001-8>.



- [3] N.Tessler, V.Medvedev, M.Kazes, S.H.Kan and U.Banin, Efficient Near-Infrared Polymer Nanocrystal Light-Emitting Diodes, *Science*, Vol. 295, No. 5559, 2002, pp. 1506–1508.
- [4] S.Kim, H.Moon, D.Gupta, S.Yoo and Y.K.Choi, Resistive Switching Characteristics of Sol-gel Zinc Oxide Films for Flexible Memory Applications, *IEEE Transaction on Electronic Devices*, Vol. 56, No. 4, 2009, pp. 696–699.
- [5] S.M.Moghimi, A.C.Hunter and J.C.Murray, Nanomedicine: Current Status and Future Prospects, *FASEB Journal*, Vol. 19, No.3, 2005, pp. 311–330.
- [6] X.Liang, M.Sun, L.Li, R.Qiao, K.Chen, Q.Xiao and F.Xu, Preparation of Antibacterial Activities of Polyaniline/Cu<sub>0.05</sub>Zn<sub>0.950</sub> Nanocomposites, *Journal of Chemical Society, Dalton Transactions*, Vol. 41, No. 9, 2012, pp. 2804–2811, <http://dx.doi.org/10.1039/c2dt11823h>.
- [7] M.R.Bindhu and M.Umadevi, Antibacterial and Catalytic Activities of Green Synthesized Silver Nanoparticles, *Spectrochimica Acta Part A: Molecular and Biomolecular Spectroscopy*, vol. 135, 2015, pp. 373–378.
- [8] P.K.Stoimenov, R.L.Klinger, G.L.Marchin and K.Klabunde, Metal Oxide Nanoparticles as Bacterial Agents, *Langmuir*, Vol. 18, No. 17, 2002, pp. 6679–6686, <http://dx.doi.org/10.1021/la0202374>.
- [9] T.Pandiyarajan, R.Udayabhaskar, S.Vignesh, R.Arthur James and B.Karthikeyan, Synthesis and Concentration Dependent Antibacterial Activities of CuO Nanoflakes, *Materials Science and Engineering: C*, Vol. 33, No. 4, 2013, pp. 2020–2024.
- [10] I.R.Kamrupi and S.K.Dolui, Synthesis of Copper–Polystyrene Nanocomposite Particles using Water in Supercritical Carbon Dioxide Medium and its Antimicrobial Activity, *Journal of Applied Polymer Science*, Vol. 120, No. 2, 2011, pp. 1027–1033.
- [11] M.A.Gondal, M.A.Dastageer, A.Khalil, K.Hayat and Z.H.Yamani, Nanostructured ZnO Synthesis and its Application for Effective Disinfection of Escherichia Coli Micro Organism in Water, *Journal of Nanoparticle Research*, Vol. 133, No. 8, 2011, pp. 423–430, <https://dx.doi.org/10.1007/s11051-011-0264-8>.
- [12] T. Kavitha and H.Yuvaraj, A Facile Approach to the Synthesis of High-Quality NiO nanorods: Electrochemical and Antibacterial Properties, *Journal of Materials Chemistry*, Vol. 21, No. 39, 2011, pp. 15686–15691, <https://dx.doi.org/10.1039/C1JM13278D>.
- [13] H.Zhang and G.Chen, Potent Antibacterial Activities of Ag/TiO<sub>2</sub> Nanocomposite Powders Synthesized by a One-Pot Sol-Gel Method, *Environmental Science and Technology*, Vol. 43, No.8, 2009, pp. 2905–2910.
- [14] M.S.Hassana, T.Amna, O.B.Yang, M.H.E.Newehy, S.S.A.Deyab and M.S.Khil, Smart Copper Oxide Nanocrystals: Synthesis, Characterization, Electrochemical and Potent Antibacterial Activity, *Colloids and Surfaces B: Biointerfaces*, Vol. 97, 2012, pp. 201–206.
- [15] W.Lou, Y.Dong, H.Zhang, Y.Jin, X.Hu, J.Ma, J.Liu and G.Wu, Preparation and Characterization of Lanthanum-Incorporated Hydroxyapatite Coatings on Titanium Substrates, *International Journal of Molecular Sciences*, Vol. 16, 2015, pp. 21070–21086.
- [16] M.I.Ahymah Joshy, K.Elayaraja, R.V.Suganthi, S.Chandra Veerla and S.N.Kalkura, In Vitro Sustained Release of Amoxicillin from Lanthanum Hydroxyapatite Nano Rods, *Current Applied Physics*, Vol. 11, No. 4, 2011, pp. 1100–1106.
- [17] V.Sarath Chandra, G.Baskar, R.V.Suganthi, K.Elayaraja, M.I.A.Joshy, W.S.Beaula, R.Mythili, Ganesh Venkatraman and S.Narayana Kalkura, Blood Compatibility of Iron-Doped Nanosize Hydroxyapatite and its Drug Release, *ACS Applied*

- Materials and Interfaces, Vol. 4, No. 3, 2012, pp. 1200–1210.
- [18] A.Doat, M.Fanjul, F.Pelle, E.Hollande and A.Lebugle, Europium-Doped Bioapatite: A New Photostable Biological Probe, Internalizable by Human Cells, *Biomaterials*, Vol. 24, No. 19, 2003, pp. 3365–3371.
- [19] B.Basar, A.Tezcaneer, D.Keskin, and Z.Evis, Improvements in Microstructural, Mechanical, and Biocompatibility Properties of Nano-Sized Hydroxyapatites Doped with Yttrium and Fluoride, *Ceramics International*, Vol. 36, No. 5, 2010, pp. 1633–1643.
- [20] I.Kostova, I.Manolov, I.Nicolova, S.Konstantinov and M.Karaivanova, New Lanthanide Complexes of 4-Methyl-7-Hydroxycoumarin and their Pharmacological Activity, *European Journal of Medicinal Chemistry*, Vol. 36, No. 4, 2001, pp. 339-347.
- [21] J.Hong-Bing, H.Xiao-Fang, S.Dong-Po and L.Zhong, Controllable Oxidation of Sulfides to Sulfoxides and Sulfones with Aqueous Hydrogen Peroxide in the Presence of  $\beta$ -Cyclodextrin, *Russian Journal of Organic Chemistry*, Vol. 42, No. 7, pp. 959-961, <http://dx.doi.org/10.1134/S1070428006070049>.]
- [22] F. Wei, D.S. Zhan, Y.Y. Wang, Differential Study of the Bonding Characterization of Dental Porcelain to Ni-Cr Alloys, *West China Journal of Stomatology*, Vol. 26, No. 5, 2008, pp. 466-469.
- [23] Y.J. Ou, Y.P. Wu, H.X. Li, K.J. Wang, D.Y. Zhang, Synthesis, Characterization and Antibacterial Activity of Hybrid Materials of Rare Earth and Chitosan, *Journal of Chinese Society Rare Earths*, Vol. 31, No. 2, 2013, pp. 211-216.
- [24] S.Suresh, P.Saravanan, K.Jayamoorthy, S.Ananda Kumar and S.Karthikeyan, Development of Silane Grafted ZnO Core Shell Nanoparticles Loaded Diglycidyl Epoxy Nanocomposites Film for Antimicrobial Applications, *Material Science and Engineering: C*, Vol. 64, 2016, pp. 286-292.
- [25] S.Suresh, S.Karthikeyan, P.Saravanan, K.Jayamoorthy and K.I.Dhanalekshmi, Comparison of antibacterial and antifungal activity of 5-amino-2-mercapto benzimidazole and functionalized Ag<sub>3</sub>O<sub>4</sub> nanoparticles, *Karbala International Journal of Modern Science*, Vol. 2, No. 2, 2016, pp. 129-137.
- [26] P.Saravanan, K.Jayamoorthy and S.A.Kumar, Fluorescence Quenching of APTES by Fe<sub>2</sub>O<sub>3</sub> Nanoparticles–Sensor and Antibacterial Applications, *Journal of Luminescence*, Vol. 178, 2016, pp. 241–248, <http://dx.doi.org/10.1016/j.jlumin.2016.05.031>.
- [27] B.Subash, B.Krishnakumar, M.Swaminathan and M.Shanthi, Highly Efficient, Solar Active, and Reusable Photocatalyst: Zr-Loaded Ag–Zno for Reactive Red 120 Dye Degradation with Synergistic Effect and Dye-Sensitized Mechanism, *Langmuir*, Vol. 29, No. 3, pp. 939-949.
- [28] B.Subash, A.Senthilraja, P.Dhatshanamurthi, M.Swaminathan and M.Shanthi, Solar Active Photocatalyst for Effective Degradation of RR 120 with Dye Sensitized Mechanism, *Spectrochimica Acta Part A: Molecular and Biomolecular Spectroscopy*, Vol. 115, 2015, pp. 175-182, <http://dx.doi.org/10.1016/j.saa.2013.06.027>.
- [29] R.Reisfeld, M.Gaft, G.Boulon, C.Panczer and C.K.Jorgensen, Laser-Induced Luminescence of Rare-Earth Elements in Natural Fluor-Apatites, *Journal of Luminescence*, Vol. 69, No. 5, 1996, pp. 343–353, [http://dx.doi.org/10.1016/S0022-2313\(96\)00114-7](http://dx.doi.org/10.1016/S0022-2313(96)00114-7).
- [30] R.Sasikala, S.Kutti Rani, D.Easwaramoorthy and K.Karthikeyan, Lanthanum :Loaded CuO Nanoparticles: Synthesis and Characterization of a Recyclable Catalyst for the Synthesis of 1,4-Disubstituted 1,2,3-Triazoles and Propargylamines, *RSC Advances*, Vol. 5, 2015, pp. 56507–56517,

- <http://dx.doi.org/10.1039/C5RA05468K>.
- [31] R.Srivastava, M.U.A.Prathap and R.Kore, Morphologically Controlled Synthesis of Copper Oxides and their Catalytic Applications in the Synthesis of Propargylamine and Oxidative Degradation of Methylene Blue, Colloids and Surfaces A: Physicochemical and Engineering Aspects, Vol. 392, No.1, 2011, pp. 271–282.
- [32] B.Subash, B.Krishanakumar, R.Velmurugan, M.Swaminathan and M.Shanthi, Synthesis of Ce Co-Doped Ag-ZnO Photocatalyst with Excellent Performance for NBB Dye Degradation under Natural Sunlight Illumination, Catalysis Science and Technology, Vol. 2, No. 11, 2012, pp. 2319–2326.
- [33] N.K.Divya and P.P.Pradyumnan, Solid State Synthesis of Erbium Doped ZnO with Excellent Photocatalytic Activity and Enhanced Visible Light Emission, Materials Science in Semiconductor Processing, Vol. 41, 2016, pp. 428–435.
- [34] K.Rekha, M.Nirmala, M.G.Nair and A.Anukaliani, Structural, Optical, Photocatalytic and Antibacterial Activity of Zinc Oxide and Manganese Doped Zinc Oxide Nanoparticles, Physica B: Condensed Matter, Vol. 405, No. 15, 2010, pp. 3180-3185.
- [35] M.Ahamed, H.A.Alhadlaq, M.A.M.Khan, P.Karupiah and N.A.Al-Dhabi, Synthesis, Characterization and Antimicrobial Activity of Copper Oxide Nanoparticles, Journal of Nanomaterials, Vol. 2014, 2014, pp. 860-865, <http://dx.doi.org/10.1155/2014/637858>
- [36] Rawoof Naikoo, Renu Tomar, Muzzaffar Mir, Samiullah Bhat and Radha Tomar, Sorption and Desorption of  $UO_2^{2+}$ ,  $Th^{4+}$ ,  $Eu^{3+}$ ,  $Ru^{3+}$  and  $Fe^{3+}$  on the Synthetic Analogue of Nepheline, DJ Journal of Engineering Chemistry and Fuel, Vol. 1, No. 1, 2016, pp. 15-16, <http://dx.doi.org/10.18831/djchem.org/2016011002>
- [37] S.Suganthi, V.Kannappan and V.Sathyanarayanamoorthi, Quantum Mechanical Studies on Free Energy of Solution of some Vitamins and their Correlation with Bioavailability, DJ Journal of Engineering Chemistry and Fuel, Vol. 1, No. 1, 2016, pp. 1-14, <http://dx.doi.org/10.18831/djchem.org/2016011001>

## APPENDIX A

Table A1. Antibacterial activity of synthesized NPs against various gram negative bacterial pathogens

Bacteria species	Zone of inhibition (mm)				
	CO	LCO	CCO	ECO	Amoxycillin
E. coli	18	23	21	22	26
P. aeruginosa	-	-	-	-	10
S. typhimurium	23	30	29	29	32
P. mirabilis	22	34	33	34	35
A. baumannii	-	-	-	-	19
K. pneumonia	11	13	10	12	20

Table A2. Minimum inhibitory concentration of synthesized NPs against different microbes ( $\mu\text{g}/\text{ml}$ )

Organism	CO	LCO	CCO	ECO
E.coli	210	75	80	80
P. aeruginosa	256	256	256	256
S.typhimurium	210	70	75	75
P. mirabilis	215	70	70	70
A.baumannii	256	256	256	256
K.pneumoniae	256	180	200	190



APPENDIX B

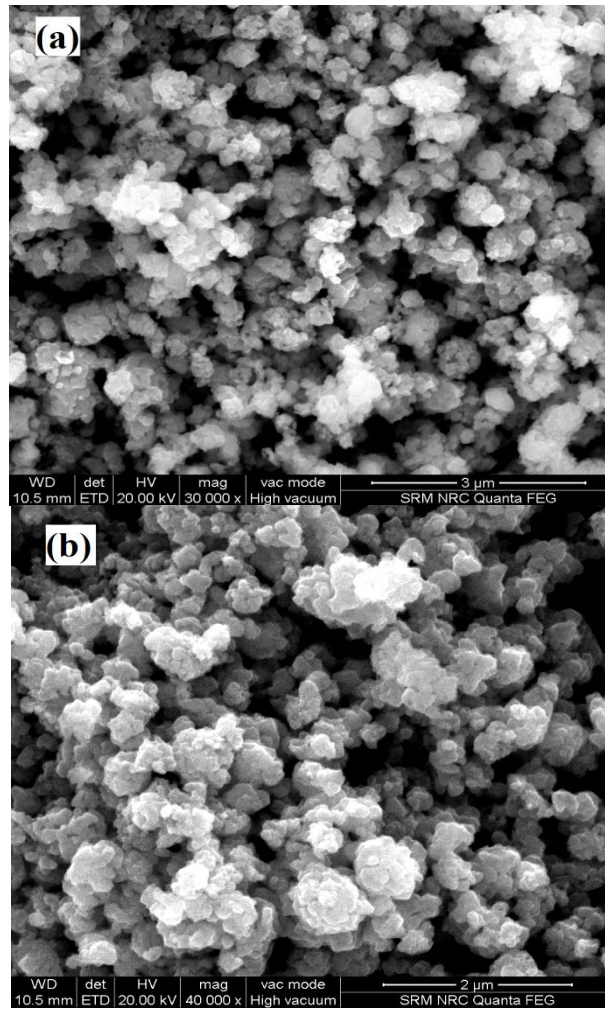


Figure B1.FE-SEM images of a) CCO (3μm), b) ECO NPs(2μm)

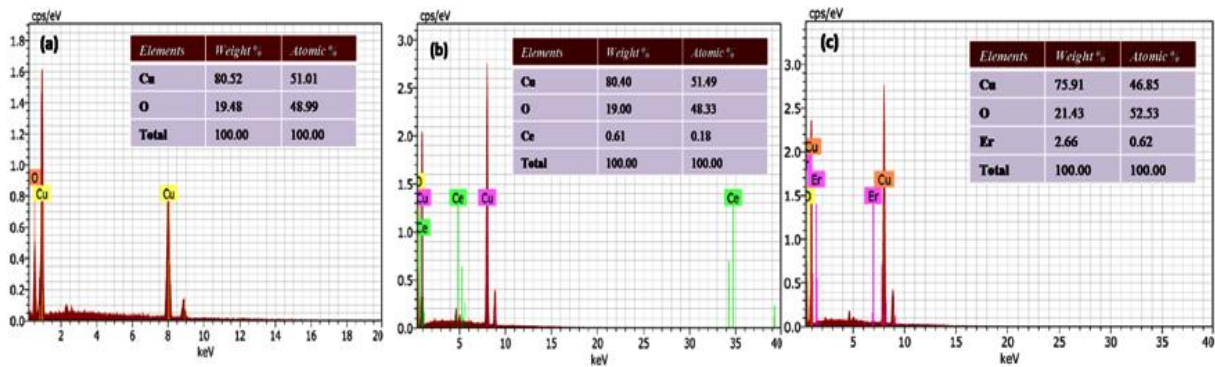


Figure B2.EDS of a) pure CuO, b) CCO and c) ECO NPs.